End Loss from a High-Beta Plasma Column

F. Brunel, T. Tajima, J. N. Leboeuf, and J. M. Dawson
Physics Department, University of California, Los Angeles, California 90024
(Received 12 February 1980)

The previous theoretically predicted diverging confinement time of a high-β linear sharp plasma column as $\beta \rightarrow 1$ is removed by including the magnetic tension effect near the column throats. This result explains our own simulation as well as those of Brackbill, Menzel, and Barnes, and is in good agreement with experimental values. The confinement time τ of a plasma with thickness a and length L at $\beta = 1$ is found to be $\tau = \frac{3}{4}(3/2\pi)^{1/2}(L/2c_s)(L/a)^{1/2}$.

PACS numbers: 52.55.Ez, 52.30.+r, 52.55.Pi, 52.65.+z

End losses from long linear systems such as a θ pinch and a long solenoid configuration[1] heated either by lasers, or electron[2] or ion beams are crucial to consideration of these devices as fusion reactors. There have been many proposals to reduce the end loss of the linear system, which include multiple mirrors, a tandem mirror,[3] solid endplug,[4] and rf plug.[5] However, the fundamental end-loss process of the simple long linear system particularly at high β is not yet fully understood; there has been considerable discrepancy between experimental results and theories for this case.

In most of the reactor designs for linear system, the end-loss time τ is calculated from $\tau = L/2c_s$, where L is the system length, the sound speed $c_s = (\gamma p/\rho)^{1/2}$, and γ the adiabatic constant. On the other hand, it has been theoretically argued that at high β the throat at the end, where the plasma pressure is low, would be closed by magnetic pressure,[6-10] leading to a loss rate proportional to $(1-\beta)^{-1/2}$.

In this Letter, we report our magnetohydrodynamic (MHD) simulation results indicating no divergence of τ at $\beta = 1$ and show that the surface magnetic tension at the column throats correctly accounts for this. Excellent correspondence of our theory with that of Brackbill, Menzel, and Barnes recent simulation[10] and experiments[11-14] are also obtained. We do find, however, that the size of the tension effect depends on the ratio of coulumn length to radius.

Computer simulations were carried out on a $2\frac{1}{2}$-dimensional MHD particle code[15] using the Lax-Wendroff algorithm to advance the magnetic field. Initially the plasma is a slab parallel to the confining magnetic field (the x direction) and with a sharp boundary in the y direction under pressure equilibrium. A low-density plasma exists outside the slab to maintain the MHD approximation. Particle end loss is treated simply by taking out the particles which touch the end. Because of the exact conservation of mass due to the particle nature of the code, the end-loss process is quite accurately described; the very-low-magnetic-field diffusion given by the Lax-Wendroff algorithm allows the sharp plasma boundary to be maintained throughout the simulation. The magnetic field boundary conditions are periodic in both x and y directions. As we shall see, the magnetic field should be purely in the x direction at the throat point where the plasma flow speed becomes sonic; the periodic boundary condition in the x direction is therefore justified even though the field pattern beyond the throat point is not incorporated in the model. Typical parameters for the simulation are the grid size $L_x \times L_y = 128\Delta \times 64\Delta$, the number of particles $N = 32768$, the Alfvén speed outside of the column is $2.83c_s$, the column width 16Δ, and the size of the particles $a_x = a_y = 1\Delta$, where Δ is a unit length of the grid.

Figure 1 shows the temporal change in density contours and the magnetic field intensity contours for a $\beta = 1$ case, where β is defined as the ratio of the internal plasma pressure to the total external pressure. For early times the density contours exhibit a surface modulation (area waves) of short wavelength as well as a general concave pattern due to a rarefactive wave[10] in the bulk plasma. The area waves are generated as particles are lost from ends and they propagate toward the center of the plasma. As time progresses, the most prominent area waves become of longer wavelength, eventually leading to a cigar-type shape [Fig. 1(b)], which appears to be a steady-state self-similar configuration. The width of the high-density plasma region at the end is quite narrow. On the other hand, the magnetic contours [Fig. 1(c)], or field lines show that although the magnetic field lines are narrowing at the ends, the magnetic throats remain widely

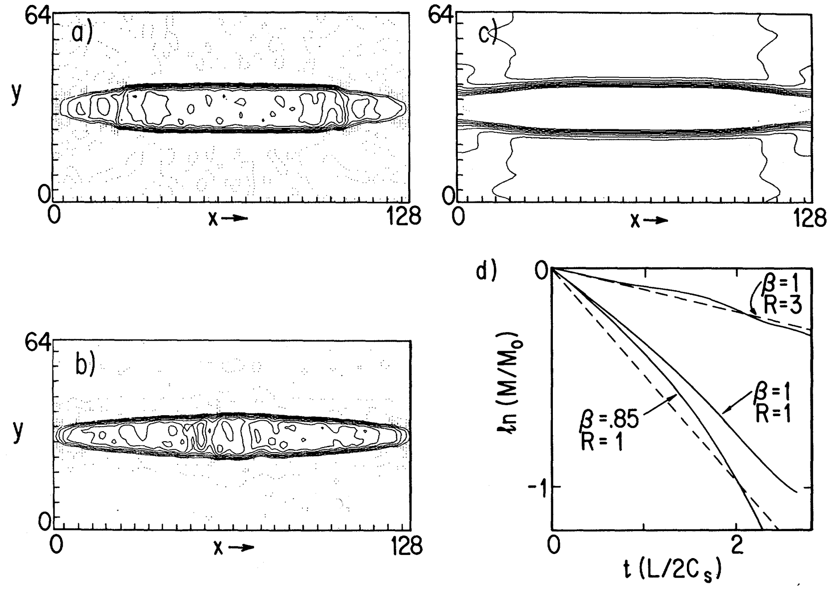

FIG. 1. (a) Density contours at $t = 40\Delta/c_s$. (b) Density contours at $t = 100\Delta/c_s$. (c) B_x^2 contours at $t = 40\Delta/c_s$. (d) Logarithm of total plasma mass vs time for $\beta = 0.8$ and $\beta = 1$.

open: The surface tension due to the magnetic field line curvature tends to open up the throat. Figure 1(d) shows a plot of the confined plasma versus time for a few cases. Even for $\beta = 1$ plasma, a finite end-loss time is observed.

We show the following (i–iii) and utilize them to derive the theoretical confinement time (end-loss time) of the high-β plasma in a linear system: (i) The plasma mass decay is exponential; (ii) the plasma flows out with a speed equal to the dominant area wave plasma velocity without a flow; (iii) the area waves propagate with nonzero velocity even at $\beta = 1$ because of the tension in the magnetic lines of force. The first (i) is actually observed to be correct in the simulation [Fig. 1(d) and Ref. 10]. The overall decay of the confined plasma is exponential in time with a small oscillatory structure superposed on it. This structure is due to transients associated with the finite length of time required to set up the steady flow. The dominant overall end loss is described by retaining only the exponential part due to the stationary fundamental as

$$L\partial_t \rho_0 a_0 = L\rho_0 a_0/\tau = -2\rho_1 a_1 u_1, \tag{1}$$

where the subscripts 0 and 1 refer to the quantities at the center of the plasma column and at the quarter point where the magnetic curvature radius becomes infinite; ρ, a, and u are plasma mass density, half-width, and fluid velocity, respectively. The second statement (ii) may be physically understood.[16] When there is no end loss and the plasma is stationary, the area waves are observed to have finite phase and group velocities even for $\beta = 1$. When there is an end flow, a stationary area wave is set up and the plasma now has to flow relative to the area wave with the same relative speed as in the former case: i.e., $u_1 = \omega/k_\parallel$, where ω and $k_\parallel$ are the area wave frequency and parallel wave number, respectively.

The area wave in the wave frame may be described by the following MHD equations:

$$\partial_x \rho u a = 0, \tag{2}$$

$$\partial_x u^2/2 + c_s^2 \rho^{-1} \partial_x \rho = 0, \tag{3}$$

$$\partial_y (p + B^2/8\pi) = B^2/4\pi R_c \tag{4}$$

$$\partial_x (aB) = 0, \tag{5}$$

where Eqs. (2)–(5) are the continuity, parallel momentum, perpendicular momentum, and flux conservation equations, respectively. R_c is the curvature radius of field lines. The right-hand side of Eq. (4) is the magnetic tension term due to the field line curvature, having been previously neglected in the end-flow theory. The x axis is taken parallel to the magnetic field. Assume a sinusoidal modulation of the boundary of the form $a(x) = a_1 - \Delta a \cos kx$, where a_1 is the half-width without end flow and Δa is the modulational amplitude. On the plasma boundary $R_c = (k^2 \Delta a \cos kx)^{-1}$.

Integrating Eq. (4) over y and differentiating it with respect to x, we obtain, with the aid of Eq. (5),

$$c_s^2 \partial_x \rho = (B^2/4\pi a)\partial_x a + (B_e^2/4\pi)\Delta a k^2 \sin kx, \qquad (6)$$

where B and B_e denote the magnetic fields inside and outside of the column. In order to integrate over y, we have used the property $\nabla^2 \psi = 0$ outside of the plasma and expanded in terms of $ka \ll 1$, where $B = \nabla\psi$. Equations (2) and (3) give rise to

$$\partial_x a = -a(1 - c_s^2/u^2)\rho^{-1}\partial_x \rho. \qquad (7)$$

Equations (6) and (7) yield the dispersion relation for area waves

$$u^2(k_\parallel) \equiv \left(\frac{\omega}{k_\parallel}\right)^2 = \frac{c_s^2(c_{Ai}^2 + c_{Ae}^2 a k_\parallel)}{c_s^2 + c_{Ai}^2 + c_{Ae}^2 a k_\parallel} = \frac{c_s^2(1 + ak_\parallel - \beta)}{1 + ak_\parallel + (\gamma - 2)\beta/2}, \qquad (8)$$

where $c_{Ai}^2 = B^2/4\pi\rho_0$ is the Alfvên speed inside the column ($c_{Ae}^2 = B_e^2/4\pi\rho_0$). The terms proportional to $ak_\parallel$ are the surface tension effect, which keeps u finite even at $\beta = 1$ in contrast to the previous theories for a sharp boundary plasma ($u = 0$ at $\beta = 1$). This dispersion relation, Eq. (8), was checked against our simulation and found to be in good agreement.

The confinement time τ can be now evaluated by Eq. (1). u_1 is given by Eq. (8)[16] with $k_\parallel = 2\pi/L$ and ρ_1 is obtained by integrating Eq. (3) as for ($\gamma = 1$)

$$\rho_1 = \rho_0 \exp(-u_1^2/2c_s^2). \qquad (9)$$

To relate a_1 to a_0, Eq. (4) is employed:

$$\rho_1 + B_1^2/8\pi = B_e^2/8\pi, \qquad (10)$$

$$\rho_0 + B_0^2/8\pi = B_e^2/8\pi + k\,\Delta a\, B_e^2/8\pi, \qquad (11)$$

where $\Delta a = a_0 - a_1$. The nozzle conditions[7] do not have to be enforced because they should be automatically adjusted to the surface-wave conditions. In fact, the nozzle conditions cannot influence the behavior inside because the flow at the end is equal to the sound speed [Eq. (7) yields $u = c_s$, where $\partial_x a = 0$ for sharp boundaries] and signals propagating with c_s just sit at the end.

The normalized confinement time $\eta = 2c_s\tau/L = a_0\rho_0 c_s/a_1\rho_1 u_1$ can be calculated by combining Eqs. (8)–(11):

$$\rho_0[1 - \exp(-u_1^2/2c_s^2)] - (B_0^2/8\pi)(a_0^2/a_1^2 - 1) = k(a_0 - a_1)B_e^2/4\pi, \qquad (12)$$

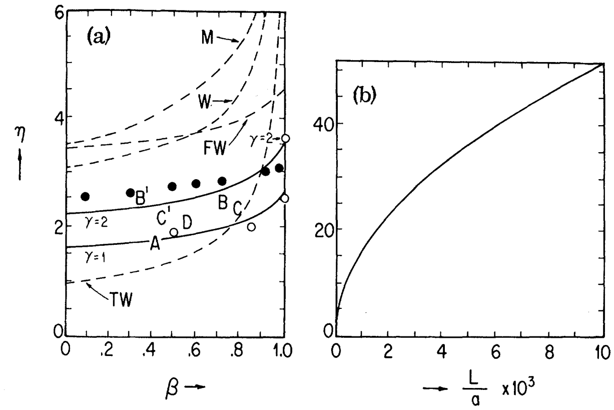

FIG. 2. (a) Confinement time η vs β. Open circles, our simulations ($\gamma = 1, 2$); dots, simulations of Brackbill, Menzel, and Barnes; real lines, our theory; broken lines with labels TW, W, M, and FW are theories of Refs. 6–9, respectively; the letters A, B, C, and D are experiments from Refs. 11–14, respectively. (b) Confinement time η vs aspect ratio L/a.

with u_1 given by Eq. (8). Numerical solutions of Eq. (12) are displayed in Fig. 2. Our simulation results as well as those of Brackbill, Menzel, and Barnes[10] fit very well with our theory [Fig. 2(a)]; experimental values roughly fall between our $\gamma = 1$ and $\gamma = 2$ curves. Figure 2(b) shows the aspect-ratio (L/a) dependence of the confinement time. When $1 - \beta \lesssim (16\pi/15)(a/L)$ and $L/a \gg 1$, we can expand the left-hand side of Eq. (12) and obtain the scaling law

$$\eta = \tfrac{3}{4}(3/2\pi)^{1/2}(L/a)^{1/2}, \qquad (13)$$

in good agreement with Fig. 2(b). When $L/a = 10^3$ at $\beta = 1$, $\eta \sim 16.5$, about an order of magnitude larger than a simple estimate, although η rapidly decreases as β decreases. For $\beta \ll 1$, $\eta \to e^{1/2}(1 + C\beta)$.

We also carried out simulations which included externally imposed mirrors. In these simulations, addition of mirror fields at the throats increases the confinement time roughly in proportion to the mirror ratio R without plasma, i.e., $\eta \propto R$.

An important question regarding the use of high β to reduce end losses from such systems is whether or not it is realistic to assume $1 - \beta$ can be made smaller than $3.4a/L$. We note there that in experiments on laser-heated solenoids $\beta \approx 1$ is achieved.[17] However, as the column starts to expand the absorption will rapidly drop so that an appreciable expansion of the column and reduction of the internal field is not possible. Maintaining the column diameter and density and hence absorption by raising the external magnetic field as the plasma pressure rises could result in high-β plasma with use of the laser heating concept. Another possibility would be to heat the column with particle beams whose rate of energy deposition drops only as density n rather than n^2. In this case one might be able to heat and inflate the central section of the plasma column like inflating a balloon, achieving large self-mirror ratios. In this regard we might point that heating the plasma with moderately heavy ion beams of 1 MeV/nucleon seems possible. The range of an ion of charge Ze, mass M, and energy W in a plasma with electron temperature T_e (in electron-volts) and electron density n_e is roughly equal to $l = 4\times 10^{11} T_e^{3/2} W^{1/2}(M/m_e)^{1/2}/Z^2 n_e$. If we consider a 1-MeV Ne ion stopping in a 10 keV plasma of density 5×10^{16}, we obtain a range of 8×10^4 cm, which is not an unreasonable length for a long linear system. To heat the plasma to 10 keV would require that we inject 3% Ne which is not an unacceptable level for totally striped Ne (effective Z of 3). To achieve this heating requires 20 MJ/cm^2 in about 2 msec if we assume a loss time of $\tau \simeq (L/2c_s)\times 10$. We would require an ion beam of 10^4 A/cm^2 of 1-MeV particles to produce this heating; the confining magnetic field would have to be 200 kG.

This work was supported by U. S. Department of Energy and National Science Foundation.

---

[1]J. M. Dawson, A. Hertzberg, R. E. Kidder, G. C. Vlases, H. G. Ahlstrom, and L. C. Steinhauer, in *Proceedings of the Fourth International Conference on Plasma Physics and Controlled Nuclear Fusion Research, Madison, Wisconsin, 1971* (International Atomic Energy Agency, Vienna, 1972), Vol. 1, p. 673.

[2]For example, T. Tajima, Ph.D. thesis, University of California, Irvine, Cal., 1975 (unpublished).

[3]T. K. Fowler and B. G. Logan, Comments Plasma Phys. Controlled Fusion 2, 167 (1977).

[4]R. J. Commissio *et al.*, Phys. Rev. Lett. 43, 442 (1979).

[5]T. Watari *et al.*, Phys. Fluids 21, 2076 (1978).

[6]J. B. Taylor and J. A. Wesson, Nucl. Fusion 5, 159 (1965).

[7]J. A. Wesson, in *Proceedings of the Second International Conference on Plasma Physics and Controlled Nuclear Fusion Research, Culham, England, 1965* (International Atomic Energy Agency, Vienna, 1966), Vol. 1, p. 223.

[8]R. L. Morse, Phys. Fluids 11, 1558 (1968).

[9]J. P. Freidberg and H. Weitzner, Nucl. Fusion 15, 217 (1975). A finite loss rate obtained for $\beta = 1$, when a diffuse boundary effect is taken into account as shown in Fig. 2.

[10]J. P. Brackbill, M. T. Menzel, and D. C. Barnes, in *Proceedings of the Third Topical Conference on Pulsed High-Beta Plasmas, Culham, England, 1975*, edited by D. E. Evans (Pergamon, New York, 1976), p. 345.

[11]K. S. Thomas, H. W. Harris, F. C. Jahoda, G. A. Sawyer, and R. E. Siemon, Phys. Fluids 17, 1314 (1975).

[12]R. F. Gribble, W. E. Quinn, and R. E. Sieman, Phys. Fluids 14, 2042 (1979).

[13]K. F. McKenna and T. M. York, Phys. Fluids 20, 1556 (1977).

[14]K. F. McKenna *et al.*, Los Alamos Scientific Laboratory Report No. LAUR 78-1909, 1978 (unpublished).

[15]J. N. Leboeuf, T. Tajima, and J. M. Dawson, J. Comput. Phys. 31, 379 (1979).

[16]More rigorous treatment to be reported by F. Brunel and T. Tajima.

[17]G. C. Valses *et al.*, in *Proceedings of the Fifth International Conference on Plasma Physics and Controlled Nuclear Fusion Research, Tokyo, Japan, 1974* (International Atomic Energy Agency, Vienna, 1975), Vol. 3, p. 197.